Organic & Biomolecular Chemistry

PAPER

View Article Online
View Journal | View Issue

Cite this: *Org. Biomol. Chem.*, 2014, **12**, 8919

Structures, chemotaxonomic significance, cytotoxic and Na^+,K^+-ATPase inhibitory activities of new cardenolides from *Asclepias curassavica*†

Rong-Rong Zhang,[a] Hai-Yan Tian,[a] Ya-Fang Tan,[a] Tse-Yu Chung,[b] Xiao-Hui Sun,[a] Xue Xia,[a] Wen-Cai Ye,[a] David A. Middleton,[c] Natalya Fedosova,[d] Mikael Esmann,*[d] Jason T. C. Tzen*[b] and Ren-Wang Jiang*[a]

Received 22nd July 2014,
Accepted 17th September 2014

DOI: 10.1039/c4ob01545b

www.rsc.org/obc

Five new cardenolide lactates (**1–5**) and one new dioxane double linked cardenolide glycoside (**17**) along with 15 known compounds (**6–16** and **18–21**) were isolated from the ornamental milkweed *Asclepias curassavica*. Their structures were elucidated by extensive spectroscopic methods (IR, UV, MS, 1D- and 2D-NMR). The molecular structures and absolute configurations of **1–3** and **17** were further confirmed by single-crystal X-ray diffraction analysis. Simultaneous isolation of dioxane double linked cardenolide glycosides (**17–21**) and cardenolide lactates (**1–5**) provided unique chemotaxonomic markers for this genus. Compounds **1–21** were evaluated for the inhibitory activities against DU145 prostate cancer cells. The dioxane double linked cardenolide glycosides showed the most potent cytotoxic effect followed by normal cardenolides and cardenolide lactates, while the C21 steroids were non-cytotoxic. Enzymatic assay established a correlation between the cytotoxic effects in DU145 cancer cells and the K_i for the inhibition of Na^+,K^+-ATPase. Molecular docking analysis revealed relatively strong H-bond interactions between the bottom of the binding cavity and compounds **18** or **20**, and explained why the dioxane double linked cardenolide glycosides possessed higher inhibitory potency on Na^+,K^+-ATPase than the cardenolide lactate.

Introduction

Cardenolides represent a class of steroids with a five-membered lactone ring at C-17. This class of compounds bind to the extracellular surface of the housekeeping membrane protein Na^+,K^+-ATPase.[1] In recent years, the anticancer effects of this class of compounds received wide attention, and was found to be related to the modifications in the Na^+,K^+-ATPase signalosome and the subsequent multiple downstream signaling pathways.[2]

Asclepias curassavica L. (commonly called Mexican butterfly weed or tropical milkweed) is a species of flowering plant in the milkweed family Asclepiadaceae. This species is native to the American tropics. Currently, it is a common ornamental garden plant and cultivated as a source of food for butterflies worldwide.[3] This species is a rich source of cardenolides. Early phytochemical studies on this herb collected from North America was carried out 50 years ago, which resulted in the isolation of calotropin as a cytotoxic principle against the nasopharynx cancer cells.[4] Subsequent studies on this herb collected from Taiwan and Yunnan provinces of China led to the identification of a series of cardenolides and their glycosides with strong cytotoxicities against human A549 (lung carcinoma cell), MCF-7 and MDA-MB-231 (both breast carcinoma cells), and HepG2 (hepatoma cell).[5–7] In our continuous search for structurally unique and biologically interesting cardiotonic steroids from the plant kingdom, this plant cultivated in Guangdong province was chosen for phytochemical investigation. Five new cardenolide lactates (**1–5**) and one dioxane double linked cardenolide glycoside (**17**) along with 15 known compounds, *i.e.* calotropagenin (**6**),[8] 5α-card-20(22)-enolide, 11β-hydroxycorotoxigenin (**7**),[9] frugoside (**8**),[10] ascleposide (**9**),[11] calactinic acid (**10**),[12] digitoxigenin (**11**),[13] sarcostin (**12**),[14] 12-*O*-benzoyldeacylmetaplexigenin (**13**),[15] curassavoside

[a]*Institute of Traditional Chinese Medicine and Natural Products, College of Pharmacy, Jinan University, Guangzhou 510632, P. R. China. E-mail: trwjiang@jnu.edu.cn; Fax: +86-20-85221559; Tel: +86-20-85221016*
[b]*Graduate Institute of Biotechnology, National Chung-Hsing University, Taichung 40227, Taiwan, China. E-mail: tctzen@dragon.nchu.edu.tw*
[c]*Department of Chemistry, University of Lancaster, Lancaster LA1 4YB, UK. E-mail: d.a.middleton@liverpool.ac.uk*
[d]*Department of Biomedicine, Aarhus University, DK-8000 Aarhus, Denmark. E-mail: me@biophys.au.dk*

†Electronic supplementary information (ESI) available: HRESIMS, IR, UV, 1D and 2D NMR spectra of **1–5** and **17**, the dose–response curves showing inhibition of Na^+,K^+-ATPase by compounds **2**, **3**, **10** and **18** . In addition, crystallographic data of **1–3** and **17** in standard CIF. CCDC 1014923–1014926. For ESI and crystallographic data in CIF or other electronic format see DOI: 10.1039/c4ob01545b

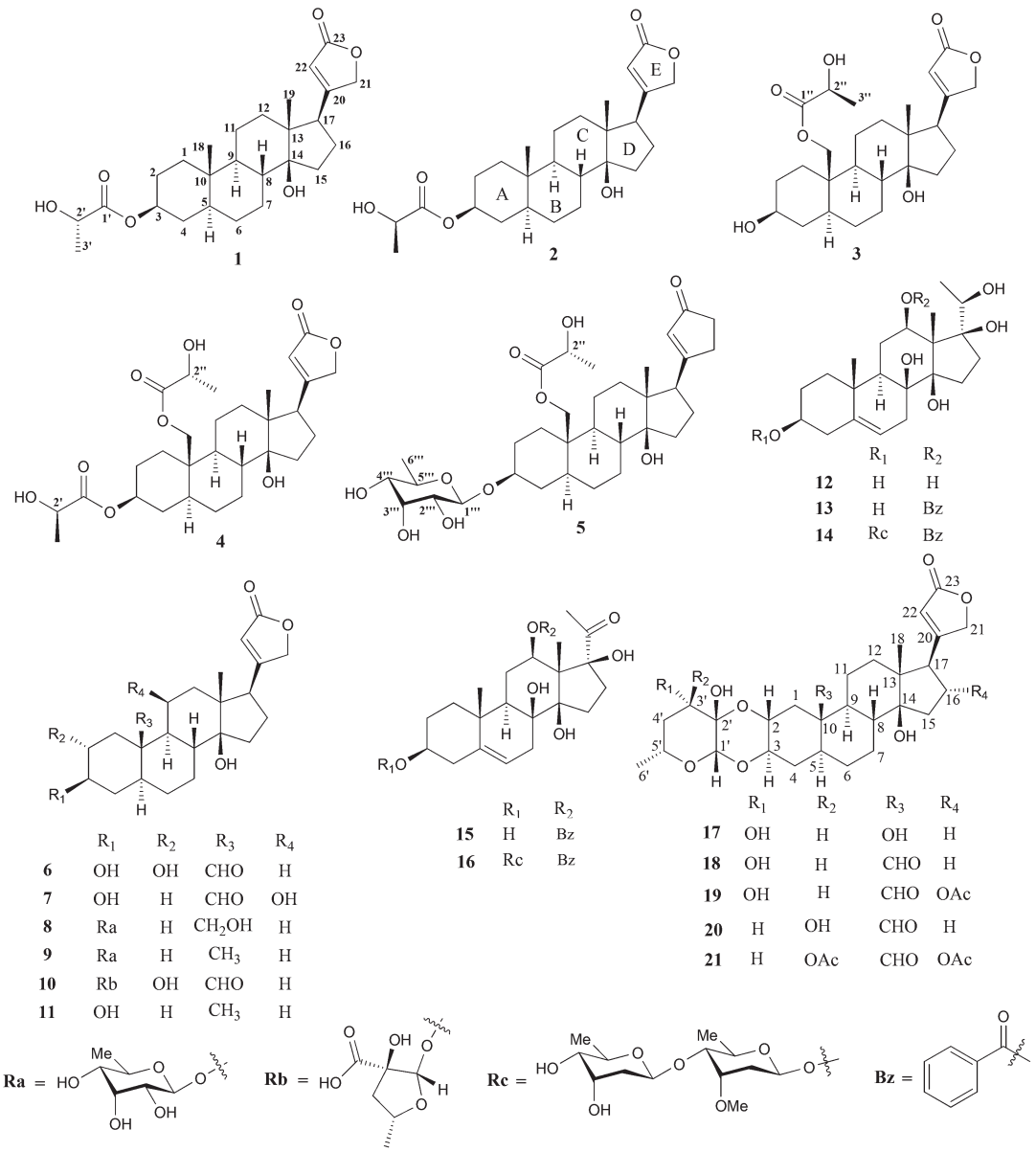

Scheme 1 Structural formulae of compounds **1–21**.

A (**14**),[15] 12-*O*-benzoylsarcostin (**15**),[15] curassavoside B (**16**),[15] calotropin (**18**),[16] 16α-acetoxycalotropin (**19**),[17] calactin (**20**)[18] and asclepin (**21**)[19] (Scheme 1), were isolated and structurally characterized by spectroscopic analysis in combination with single-crystal X-ray diffraction. Herein we report the structural elucidation, chemotaxonomic significance and biological activities of these compounds.

Results and discussion

Compound **1** was isolated as colorless crystals. HRESIMS analysis of **1** showed a quasi-molecular ion peak at *m*/*z* 469.2563 $[M + Na]^+$, corresponding to a molecular formula $C_{26}H_{38}O_6$. The IR spectrum of **1** exhibited prominent absorption bands at 3430, 1733 and 1716 cm^{-1}, indicating the presence of hydroxyl and carbonyl functionalities. ^1H and ^{13}C NMR spectra of **1** (Table 1) showed the typical signals for a butenolactone ring [δ_H 5.89 (1H, s, H-22), 4.99 (1H, dd, J = 18.4, 1.5 Hz, H-21β), and 4.94 (1H, dd, J = 18.4, 1.5 Hz, H-21α), and δ_C 177.3, 178.5, 117.8 and 75.3], two methyl singlets [δ_H 0.85 (3H, s, H-19) and 0.88 (3H, s, H-18), δ_C 12.5 and 16.4], one methyl doublet [δ_H 1.35 (3H, d, J = 6.9 Hz, H-3′), δ_C 20.6], resonances for two oxygenated carbons [δ_H 4.18 (1H, q, J = 6.9 Hz, H-2′) and 4.73 (1H, m, H-3), and δ_C 67.9 and 75.5], and an additional ester carbonyl at δ_C 176.0. The ^{13}CNMR chemical shifts of all the hydrogenated carbons could be assigned unambiguously from the HSQC spectrum. Comparison of the NMR data for **1** with desglucouzarin[20] indicated that the ^1H and ^{13}CNMR signals for the protons and carbons in the A, B, C, D and E rings had similar

Table 1 ^{1}H and ^{13}C NMR data for **1–5** and **17**

	1[a]		**2**[b]		**3**[a]		**4**[a]		**5**[a]		**17**[a]	
Position	δ_H[c]	δ_C	δ_H[c]	δ_C	δ_H[c]	δ_C	δ_H[c]	δ_C	δ_H[d]	δ_C	δ_H[d]	δ_C
1	1.07, m	37.9	0.94, m	37.1	0.92, m	32.1	0.99, m	32.4	0.94, m	32.8	1.54, m	32.9
	1.89, m		1.86, m		1.71, m		2.31, m		2.28, m		1.82, m	
2	1.25, m	29.8	1.09, m	29.00	1.19, m	29.6	1.19, m	28.5	1.19, m	29.5	3.92, m	73.3
	1.36, m		1.17, m		1.38, m		1.40, m		1.40, m			
3	4.73, m	75.5	4.93, m	74.1	3.58, m	71.1	4.79, m	74.9	3.71, m	78.7	4.21, m	70.1
4	1.43, m	34.8	1.35, m	34.3	1.35, m	38.9	1.54, m	35.0	1.43, m	35.7	1.09, m	35.2
	1.60, m		1.60, m		1.67, m		1.74, m		1.85, m		1.85, m	
5	1.52, m	45.6	0.97, m	44.4	1.09, m	45.7	1.41, m	45.5	1.32, m	45.6	1.69, m	41.7
6	1.81, m	28.6	1.89, m	28.0	1.86, m	27.9	1.86, m	28.4	1.87, m	28.5	1.60, m	28.1
	2.05, m		2.28, m		2.21, m		2.10, m		2.20, m		2.14, m	
7	1.13, m	28.4	1.09, m	27.8	1.17, m	33.2	1.18, m	29.2	1.91, m	30.5	1.46, m	28.4
	1.83, m		1.56, m		1.57, m		1.39, m		1.91, m		2.20, m	
8	1.60, m	42.5	1.38, m	41.7	1.70, m	43.0	1.71, m	43.0	1.71, m	43.0	1.50, m	40.4
9	1.01, m	50.9	0.86, m	49.8	1.34, m	51.2	1.13, m	50.5	1.11, m	50.7	1.35, m	45.0
10		36.8		36.0		39.6		39.6		39.6		75.3
11	1.53, m	22.3	1.37, m	21.6	1.28, m	24.0	1.64, m	23.7	1.29, m	23.8	1.55, m	21.9
	1.53, m		1.90, m		1.65, m		1.64, m		1.66, m		1.88, m	
12	1.49, m	40.7	1.38, m	39.7	1.47, m	41.0	1.48, m	40.9	1.48, m	41.0	1.52, m	40.5
	1.49, m		1.68, m		1.47, m		1.48, m		1.48, m		2.10, m	
13		50.9		50.1		50.7		51.0		51.0		50.9
14		86.2		84.6		86.2		86.1		86.0		86.0
15	1.71, m	33.3	1.84, m	33.3	1.71, m	32.9	1.71, m	33.4	1.71, m	33.4	1.71, m	33.3
	2.13, m		2.05, m		2.25, m		2.12, m		2.14, m		2.11, m	
16	1.84, m	27.9	1.56, m	27.4	1.71, m	28.4	1.62, m	27.9	1.87, m	28.0	1.89, m	27.9
	2.15, m		2.05, m		2.12, m		2.12, m		2.13, m		1.99, m	
17	2.81, m	52.0	2.78, m	51.5	2.82, m	51.9	2.83, m	51.9	2.83, m	52.0	2.80, m	52.0
18	0.87, s	16.4	1.00, m	16.3	0.86, s	16.4	0.88, s	16.4	0.86, s	16.4	1.22, s	16.3
19	0.85, s	12.5	0.69, m	12.2	4.27, d (12.2)	63.5	4.34, m	63.2	4.31, m	63.4		
					4.42, d (12.2)		4.43, m		4.41, m			
20		178.4		174.6		178.3		178.3		178.3		178.4
21	4.94, dd (18.4, 1.5)	75.4	5.02, dd (18.4, 1.5)	73.8	4.89, dd (18.4, 1.5)	75.4	4.90, dd (18.6, 1.5)	75.3	4.90, brd (19.1)	75.3	4.90, dd (17.6, 1.5)	74.0
	4.99, dd (18.4, 1.5)		5.30, dd (18.4, 1.5)		5.00, dd (18.4, 1.5)		5.02, dd (18.6, 1.5)		5.02, brd (18.5)		5.03, dd (17.6, 1.5)	
22	5.89, s	117.8	6.12, s	117.8	5.89, s	117.5	5.89, s	117.8	5.89, s	117.8	5.89, s	117.8
23		177.2		176.1		177.2		177.2		177.2		177.2
1′		176.0		175.5				175.9				
2′	4.21, q (6.9)	67.9	4.66, q (6.8)	67.7			4.19, q (6.9)	67.9				
3′	1.35, d (6.9)	20.6	1.65, d (6.8)	21.3			1.34, d (6.9)	20.6				
1″						176.3		176.3		176.4		
2″					4.42, m	67.9	4.25, m	67.9	4.42, m	67.8		
3″					1.37, d (6.9)	20.6	1.37, d (7.0)	20.5	1.36, d (6.9)	20.5		
1‴									4.71, d (8.0)	99.8	4.45, s	97.4
2‴									3.24, dd (7.9, 2.8)	72.4		92.6
3‴									4.0, t (2.9)	72.8	3.58, dd (12.1, 4.7)	74.0
4‴									3.13, dd (9.5, 2.7)	74.3	1.71, m	39.6
											1.71, m	
5‴									3.72, m	70.5	3.65, m	69.4
6‴									1.21, d (6.2)	18.2	1.22, d (6.1)	21.3

[a] ^{1}H and ^{13}C NMR data were recorded in methanol-d_4 (δ in ppm J in Hz). [b] ^{1}H and ^{13}C NMR data were recorded in pyridine-d_5 (δ in ppm J in Hz). [c] ^{1}H NMR data were obtained on 300 MHz spectrometers. [d] ^{1}H NMR data were obtained on 400 MHz spectrometers.

chemical shifts. The major differences in the ^{13}C NMR spectral data between **1** and desglucouzarin[20] were the presence of a lactate unit (one carbonyl, one oxygenated methine and one methyl) in **1** instead of a sugar unit in desglucouzarin.[21]

The full NMR data assignments of **1** were determined by the analyses of ^{1}H–^{1}H COSY, HSQC and HMBC spectroscopic data (Fig. 1). The ^{1}H–^{1}H COSY spectrum showed three spin coupling systems (in bold face in Fig. 1): (i) H_2-1 → H_2-2 → H-3 → H_2-4 → H-5 → H_2-6 → H_2-7 → H-8 → H-9 → H_2-11 → H_2-12, (ii) H_2-15 → H_2-16 → H-17, and (iii) H_3-3′ → H-2′, which were consistent with the cardenolide lactate skeleton. The HSQC spectrum revealed that the proton at δ_H 5.89 (H-22) was attached to the carbon at δ_C 117.8 (C-22), and the HMBC spectrum showed that H-22 was correlated to C-20, C-21, and C-23, suggesting that the furan-2(5*H*)-one unit could be formed by ring closure involving an oxygen atom bridged to C-21 and C-23. Specially, HMBC correlations from H_3-3′ (δ_H 1.35) to C-2′ (δ_C 67.9) and C-1′ (δ_C 176.0), confirmed the presence of a lactate unit in compound **1**, and the correlation between H-3 [δ_H 4.73 (1H, m)] and C-1′ established location of the lactate unit at C-3. Taken together, compound **1** was determined as a new cardenolide with a lactate moiety at C-3 as shown in Fig. 1.

The relative configuration of **1** was determined by analysis of NOESY data, which showed correlations H_3-19 ↔ H-8, H-8 ↔ H_3-18, indicating that H_3-19, H-8 and H_3-18 were the same β-oriented. Similarly, the NOESY correlations H-3 ↔ H-5, H-5 ↔ H-9, but absence of correlation H-3 ↔ H_3-18 suggested that H-3, H-5, H-9 were mutually oriented on the other side.

In spite of the above NOESY correlation data, we were unable to assign the configuration of C-2′ in the lactate unit. Fortunately, crystals suitable for X-ray diffraction analysis were obtained from methanol solution of **1**. Final refinement of the CuKα diffraction data resulted in a small Flack parameter 0.1(2), allowing the assignment of the absolute configuration (Fig. 2). Accordingly, the structure of compound **1** was established as (3*S*,5*S*,8*R*,9*S*,10*S*,13*R*,14*S*,17*R*,2′*S*)-3-*O*-urarigeninlactate.

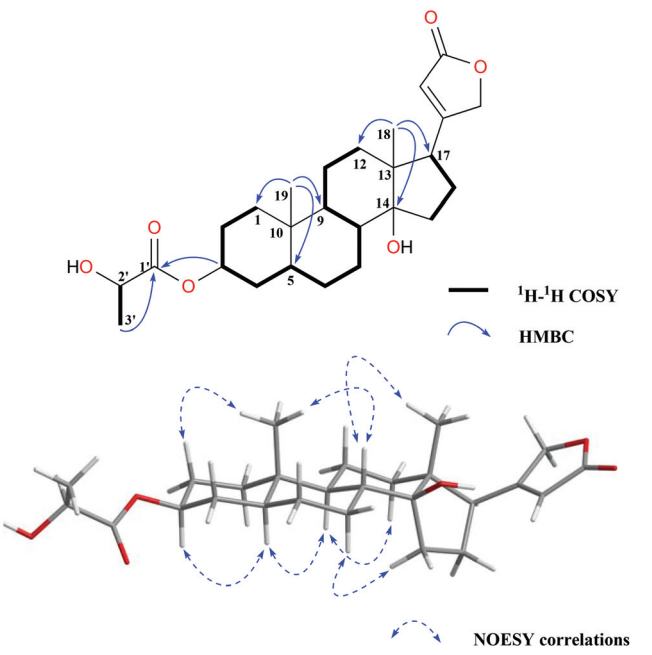

Fig. 1 Key ^{1}H–^{1}H COSY, HMBC and NOESY correlations of **1**.

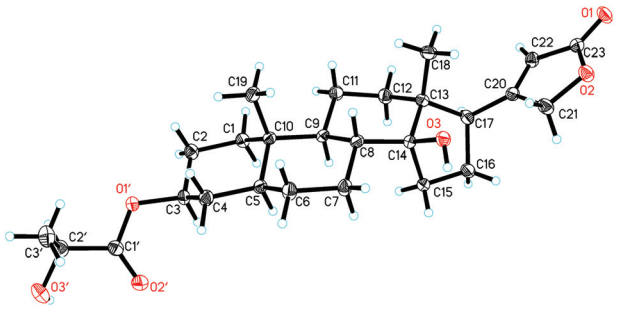

Fig. 2 X-ray structure of **1** showing the atom labeling scheme. The C and O atoms are drawn as 30% thermal ellipsoids.

Compound **2** was obtained as colorless crystals. HRESIMS analysis of **1** showed a quasi-molecular ion peak at *m*/*z* 447.2745 $[M + H]^+$, corresponding to a molecular formula $C_{26}H_{38}O_6$, which was the same as compound **1**. Its IR spectrum exhibited absorption bands for hydroxyl (3412 cm^{-1}), carbonyls (1733 cm^{-1} and 1717 cm^{-1}) functionalities. Proton signals at δ_H 4.66 (1H, q, J = 6.8 Hz, H-2′) and 1.65 (d, J = 6.8 Hz, H-3′) and carbon signals at δ_C 175.5, 67.7 and 21.3 were assignable to a lactate unit. Both the ^{1}H and ^{13}C-NMR of **2** were similar to those of **1**; however, the retention times were different (26.8 min for **1** and 27.8 min for **2**, Fig. 3), indicating that **2** was an isomer of **1**.

Crystals of **2** suitable for X-ray diffraction analysis were obtained from methanol solution. The absolute configuration of compound **2** could be unambiguously established by single crystal X-ray analysis based on the low Flack parameter −0.04 (17) (Fig. 4). Accordingly, the structure of compound **2** was established as (3*S*,5*S*,8*R*,9*S*,10*S*,13*R*,14*S*,17*R*,20*Z*,2′*R*)-3-*O*-urarigeninlactate, which is an isomer of **1** at the chiral center of the lactate unit.

The molecular formula of compound **3** was determined to be $C_{26}H_{39}O_7$ from its HRESIMS (*m*/*z* 463.2677, $[M + H]^+$). The IR spectrum indicated hydroxyl and carbonyl functionalities at 3469, 1733 and 1714 cm^{-1}, respectively. The ^{1}H- and ^{13}C-NMR (Table 1) spectra were similar to those of **2**, indicating that **3** was also a cardenolide bearing a lactate unit with proton signals at δ_H 4.42 (1H, *m*, H-2′) and 1.37 (d, J = 6.9 Hz, H-3′), and carbon signals at δ_C 176.3, 67.9 and 20.6; however, there was only one methyl group [δ_H 0.86 (3H, s, H-18); δ_C 16.4] in **3**, and the other one was replaced by an oxygenated methylene [δ_H 4.27 (H, d, J = 12.3 Hz, H-19α) and δ_H 4.42 (H, d, J = 12.3 Hz, H-19β); δ_C 63.5]. The location of the oxygenated methylene at C-19 was revealed by HMBC correlations from H_α-19 to C-1 (δ_C 32.1), C-5 (δ_C 45.7) and C-9 (δ_C 51.2) (see ESI†). Furthermore, HMBC correlations from C-1″ (δ_C 176.3) to both H-19α and H-19β indicated the location of the lactate unit at C-19. Finally the absolute configuration of **3** was confirmed by single crystal X-ray analysis (Fig. 5) with a low Flack parameter 0.17(17). Accordingly, compound **3** was determined as (3*S*,5*S*,8*R*,9*S*,10*R*,13*R*,14*S*,17*R*,20*Z*,2″*S*)-19-*O*-coroglaucigeninlactate.

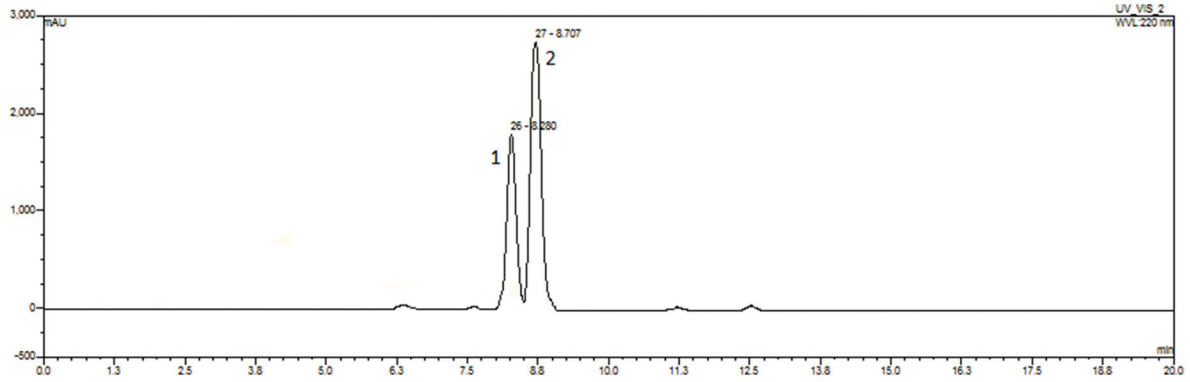

Fig. 3 Comparison of compounds **1** and **2** by HPLC. HPLC conditions: Agilent 1200 system, reverse phase C-18 column (5 μm, 20 × 250 mm; Cosmosil, Japan), mobile phase: $CH_3CN–H_2O$ (7 : 3), and detection at 220 nm.

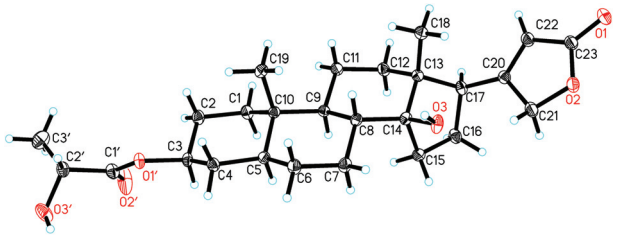

Fig. 4 X-ray structure of **2** showing the atom labeling scheme. The C and O atoms are drawn as 30% thermal ellipsoids.

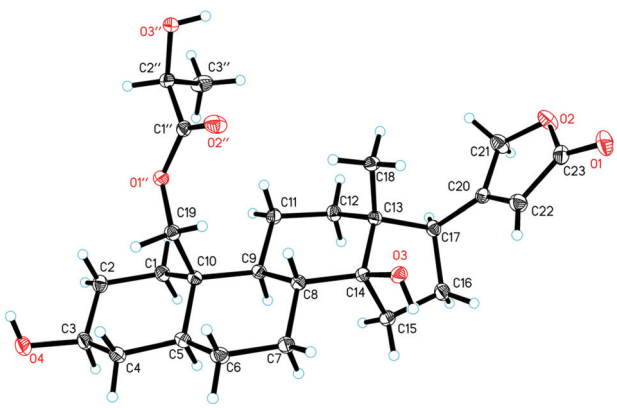

Fig. 5 X-ray structure of **3** showing the atom labeling scheme. The C and O atoms are drawn as 30% thermal ellipsoids.

Compound **4**, colorless powder, had a molecular formula $C_{29}H_{42}O_9$ as determined by HRESIMS (*m*/*z* 557.2448 $[M + H]^+$). Absorption bands at 3446, 1733 and 1711 cm^{-1} in the IR spectrum demonstrated the presence of hydroxyl and carbonyl groups, respectively. The ^{13}C NMR and DEPT spectrum contained 29 signals assigned to three methyls, eleven methylenes, eight methines, and seven quaternary carbons including four carbonyl carbons (δ_C 175.9, 176.3, 177.2 and 178.3). Comparison of the NMR data of **4** with **2** and **3** revealed that **4** was a cardenolide bearing two lactate units with signals at δ_H 4.19 (1H, q, *J* = 6.9 Hz, H-2′) and 1.37 (d, *J* = 6.9 Hz, H-3′), δ_C 175.5, 67.9 and 20.6 for one unit, and δ_H 4.25 (1H, m, H-2″) and 1.37 (d, *J* = 6.9 Hz, H-3″), δ_C 176.3, 67.9 and 20.5 for another unit. HMBC correlations between H-19 [δ_H 4.34 (1H, m, H-19α), δ_H 4.43 (1H, m, H-19β)] and C-1″ (δ_C 176.3) suggested one lactate unit at C-19. Similarly, HMBC correlation between H-3 [δ_H 4.79 (1H, m)] and C-1′ (δ_C 175.9) (see ESI†) suggested another lactate unit at C-3. In order to confirm the configuration of the lactate units at C-3 and C-19, compound **4** was hydrolyzed in a solution of NaOH in MeOH. After removing the steroid moiety, the specific optical rotation value of the aqueous solutions was −4.5°, which was consistent with the specific optical rotation value of *R*-lactic acid (−3.8°), suggesting both lactate units were the same. Accordingly, the structure of **4** was identified as (3*S*,5*S*,8*R*,9*S*,10*S*,13*R*,14*S*,17*R*,20*Z*,2′*R*,2″*R*)-coroglaucigenin-3,19-*O*-dilactate.

The molecular formula of **5** was established to be $C_{32}H_{48}O_{11}$ by analysis of its HR-ESIMS which exhibited a quasi-molecular ion at *m*/*z* 608.2531 $[M + H]^+$. Comparison of the NMR data of **5** (Table 1) with those of **3** showed that their signals for the protons and carbons in the A, B, C, D and E rings were similar, and compound **5** also has a lactate unit [δ_H 4.42 (1H, m, H-2″), 1.36 (d, *J* = 6.9 Hz, H-3″), δ_C 176.4, 67.8, 20.5] at C-19, which was confirmed by the HMBC correlation between H-19 and C-1″. In contrast, the signals for H-3 (δ_H 3.71) and C-3 (δ_C 78.7) were shifted to downfield as compared with those of **3**, suggesting that there might be a sugar unit at C-3. The characteristic signals δ_C 99.8, 72.4, 72.8, 74.3, 70.5, 18.2 suggested the presence of a rhamnose unit, which was also observed in frugoside (**8**),[10] and the coupling constant of the anomeric proton (δ_H 4.71, d, *J* = 8.0 Hz, H-1‴) suggested the β-configuration of the glycosidic bond.

The HMBC correlations between H-1‴ and C-3 further confirmed the location of the sugar unit at C-3 (see ESI†). In order to confirm the configuration of the lactate unit at C-19, similar to **4**, compound **5** was hydrolyzed in a solution of NaOH in MeOH, and the specific optical rotation value of the aqueous solutions was −3.9°, which was consistent with that of *R*-lactic acid (−3.8°). Accordingly, the structure of **5** was determined as (3*R*,5*S*,8*R*,9*S*,10*R*,13*R*,14*S*,17*R*,20*Z*,2″*R*)-19-*O*-frugosidelactate.

The molecular formula of compound **17** was deduced to be $C_{28}H_{40}O_9$ by the analysis of HR-ESIMS (*m*/*z* 521.2581 $[M + H]^+$).

Absorption bands at 3420 and 1725 cm^{-1} in the IR spectrum of **17** demonstrated the presence of hydroxyl and carbonyl groups, respectively. The ^1H NMR spectrum of the aglycone portion of **17** showed characteristic signals of a butenolactone ring at δ_H 5.89 (1H, d, J = 1.5 Hz), 4.90 (1H, dd, J = 17.6, 1.5 Hz), and 5.03 (1H, dd, J = 17.6, 1.5 Hz), as well as a methyl signal at δ 1.22 (3H, s), indicating a cardenolide skeleton with a loss of methyl at C-19. The ^{13}C NMR spectrum of **17** showed 28 carbon signals, of which 22 could be assigned to the aglycone moiety and six assigned to a sugar unit. Analysis of the ^{13}C and DEPT NMR spectra confirmed clearly the occurrence of two oxygenated quaternary carbon atoms (δ_C 75.3 and 86.0) along with signals typical of a butenolactone ring: a carbonyl group (δ 177.2), an olefinic quaternary carbon (δ_C 178.4), an olefinic methine (δ_C 117.8), and an oxygenate methylene (δ_C 74.0) in the aglycone moiety. The ^1H and ^{13}C NMR chemical shifts of the aglycone moiety of **17** were similar to those of the known compound calotropin (**18**)[16] except that the aldehyde group at C-10 of **18** was replaced with a hydroxyl group in **17**, which was further confirmed by HMBC correlations between C-10 (δ_C 75.3) and H-2 [δ_H 3.92 (1H, m)], H-5[δ_H 1.69 (1H, m)] and H-8 [δ_H 1.50 (1H, m)] (Fig. 6). Additionally, the ^1H NMR spectrum of **17** displayed a signal corresponding to an anomeric proton at δ_H 4.45 (1H, s, H-1′),[16] which suggested that **17** is a doubly linked glycoside. The relative configuration of C-3′ was established by analysis of ^1H NMR coupling constants (δ_H 3.61, dd, J = 12.1, 4.7 Hz, H-3′), which indicated an axial position and thus an *S*-configuration at C-3′.

In the NOESY spectrum, correlations H_α-1 ↔ H-5, H-5 ↔ H-9 and H-3 ↔ H-5 suggested these H_α-1, H-3, H-5 and H-9 was all α-oriented (Fig. 6). NOESY correlation H-5′ ↔ H-1′ and absence of correlations between H-1′ and H-3′ indicated that

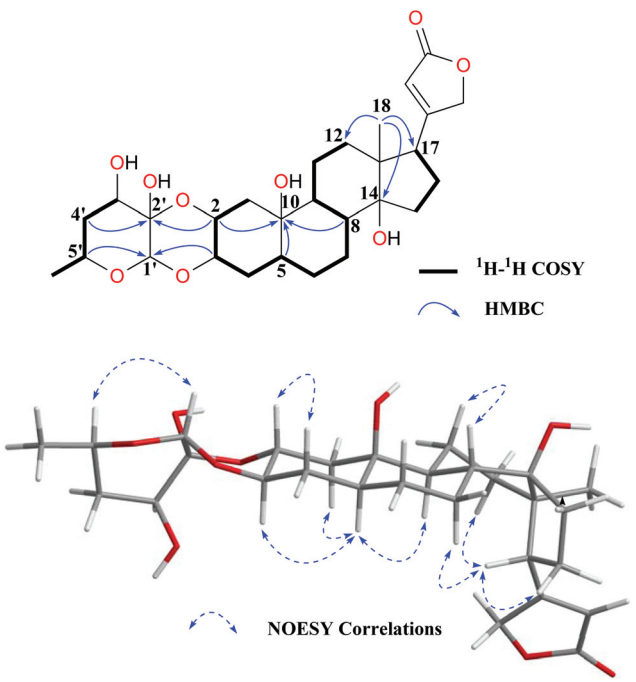

Fig. 6 Key ^1H–^1H COSY, HMBC and NOESY correlations of **17**.

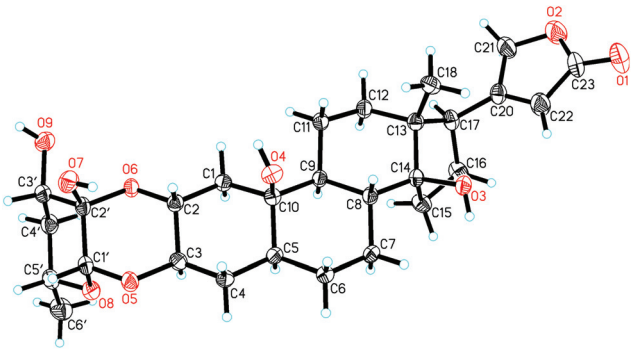

Fig. 7 X-ray structure of **17** showing the atom labeling scheme. The C and O atoms are drawn as 30% thermal ellipsoids.

H-1′ and H-5′ were β-oriented. However, the configurations of the tertiary hydroxyl group at C-10, C-14 and C-2′ could not be established by NOESY spectrum. Fortunately, single crystals were obtained from methanol solution. X-ray analysis with CuKα diffraction data resulted in a small Flack parameter 0.0 (2), which confirmed the configurations deduced from NMR analysis and revealed the configurations for the tertiary hydroxyl groups (Fig. 7). Accordingly, the structure of **17** was identified as (2*R*,3*R*,5*S*,8*R*,9*S*,10*R*,13*R*,14*S*,17*R*,20*Z*,1′*S*,2′*S*,3′*S*,5′*R*)-19β-hydroxycalotropin.

Other known compounds were identified by comparison of the physical and spectroscopic data with the literature as shown in the Introduction section. It is noteworthy that **1–5** are five new cardenolide lactates. Among them, compounds **1** and **2** have a lactate unit at C-3, the lactate unit of **3** is linked at C-19, compound **4** has two lactate units at both C-3 and C-19, while compound **5** is a cardenolide glycoside with a lactate unit at C-19. Lactic acid is widely present in the human body, animals, plants and microorganisms.[22] It is commonly used as an additive in food, drug salt, *e.g.* milrinone lactate in pharmaceutical industries,[23] and serves as a raw material for the production of biodegradable polymers.[24] However, this is the first report that natural bioconjugates of cardenolide and lactic acid exist in plants.

Cardenolides are endogenously produced in about 60 genera of 12 families of the angiosperms, for examples Asclepiadaceae and Apocynaceae families.[25] Especially, cardenolides from the Asclepiadaceae family often form a dioxane ring between the cardenolide aglycone and the sugar unit (*e.g.* compounds **17–21** in this study), particularly in genera of *Asclepias* and *Calotropis*, two close genera in the mega-tree cladogram of Apocynaceae.[25] This structure feature is rarely found in the cardenolides from other families. Simultaneous isolation of dioxane double linked cardenolide glycosides (**17–21**) and cardenolide lactates (**1–5**) provided unique chemotaxonomic markers for this genus.

MTT colorimetric assay was performed to test the inhibitory activities of **1–21** against DU145 prostate cancer cells. As shown in Table 2, the dioxane double linked cardenolide glycosides **17–21** showed the most potent cytotoxic effect against DU145 cells (IC_{50} values in the range 0.03–0.29 μM), the normal cardenolides and related glycosides **6–11** also

Table 2 Inhibitory activities against DU145 cancer cells of compounds 1–21

Compound	IC_{50}[a] (μM)	Compound	IC_{50}[a] (μM)
1	14.38 ± 2.45	**12**	>25.00
2	1.66 ± 0.13	**13**	>25.00
3	5.31 ± 0.41	**14**	>25.00
4	16.96 ± 0.89	**15**	>25.00
5	16.80 ± 1.43	**16**	>25.00
6	0.48 ± 0.08	**17**	0.29 ± 0.03
7	0.92 ± 0.09	**18**	0.03 ± 0.01
8	0.34 ± 0.06	**19**	0.28 ± 0.02
9	0.33 ± 0.05	**20**	0.04 ± 0.01
10	0.39 ± 0.04	**21**	0.21 ± 0.01
11	0.33 ± 0.05	**Taxol**[b]	0.12 ± 0.02

[a] The experiments were performed three times, each in triplicate. [b] Positive control.

demonstrated strong cytotoxic effects with IC_{50} values in the range 0.33–0.92 μM, and the cardenolide lactates **1–5** exhibited moderate cytotoxic effects with IC_{50} values in the range 1.66–16.96 μM, while the C21 steroids **12–16** were inactive with IC_{50} values larger than 25 μM.

The cytotoxic effects of cardenolides were reported to be related to the modifications in the Na^+,K^+-ATPase signalosome.[2] Thus, representative compounds **2** and **3** from the cardenolide lactate group, **8** and **10** from the normal cardenolide group and **18–21** from the dioxane double linked cardenolide glycoside group were tested for their inhibitory effects on Na^+,K^+-ATPase. As shown in Table 3, the inhibitions of Na^+,K^+-ATPase were generally consistent with the cytotoxic effects, and thus establishes a correlation between the cytotoxic effect in human cancer cells and the K_i for the inhibition of Na^+,K^+-ATPase. Particularly, compounds **8** and **18–21** showed very potent inhibitory activities with K_i values less than 0.05 μM. The dose-response curves showing inhibition of Na^+,K^+-ATPase by representative compounds were shown in Fig. S46 (ESI†).

The interactions between normal cardenolides, *e.g.* ouabain, and Na^+,K^+-ATPase have been studied by solid state NMR,[26] X-ray crystallography[27] and molecular docking analysis,[28] while interactions between the cardenolide lactates, dioxane double linked cardenolide glycosides and Na^+,K^+-ATPase have not been reported. In this study, we explored the binding modes of compounds **2**, **18** and **20** with the molecular docking approach.

Similar to the complex structure of ouabain with Na^+,K^+-ATPase,[29] the head five-membered lactone rings of compounds **2**, **18** and **20** penetrated deeply into the binding cavity (Fig. 8).

Table 3 Na^+,K^+-ATPase inhibitory activities of the representative compounds

Compounds	K_i (μM)	Compounds	K_i (μM)
2	0.163	**18**	<0.05
3	10.750	**19**	<0.05
8	<0.05	**20**	<0.05
10	0.960	**21**	<0.05
Ouabain[a]	<0.05		

[a] Positive control.

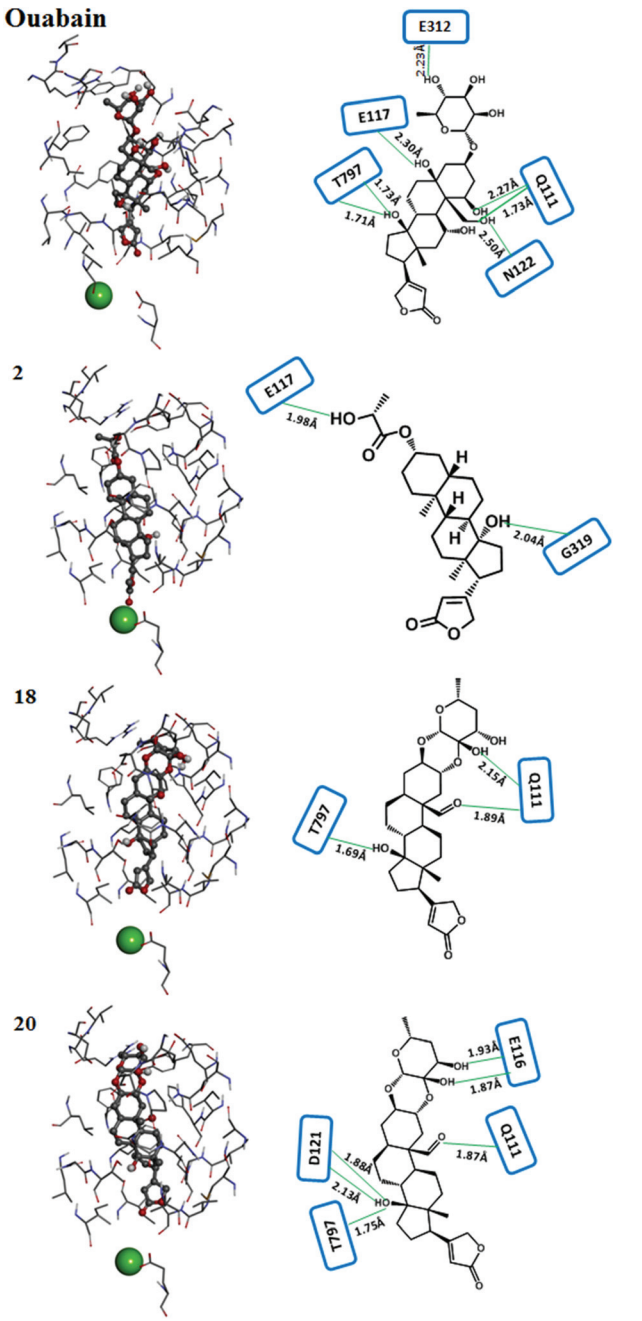

Fig. 8 Detailed molecular interactions between the binding pocket of Na^+,K^+-ATPase and compounds **2**, **18** and **20**. The binding mode of ouabain with Na^+,K^+-ATPase was shown in upper panel to depict the localization of the ouabain site. (Left panels) The amino acids of Na^+,K^+-ATPase close to the ligand compounds (ball-and-stick structure) are shown in stick structure. Mg^{2+} close to the ligand is shown in CPK (green ball). (Right panels) Interactions between Na^+,K^+-ATPase and ligand compounds are depicted in simple drawings. Amino acid residues of Na^+,K^+-ATPase involved in formation of hydrogen bonds are shown in blue squares. Distances of hydrogen bonds (green lines) between ligands and Na^+,K^+-ATPase (from donor hydrogen to receptor) are indicated. The distance between Mg^{2+} and ligands (ouabain) is rather long (about 6.4 Å), and no direct interaction was observed between Mg^{2+} and ligands (ouabain).

H-bonds were formed between the binding cavity of Na^+,K^+-ATPase and compounds **2**, **18** and **20**. In the docking simulation of compound **2**, two H-bonds were found; one was formed between the hydroxyl group at C-14 and G319 (distance 2.04 Å, all distances were shown from donor hydrogen to receptor), and the other was formed between the lactate moiety at C-3 and E117 (distance 1.98 Å). In the docking simulation of compound **18**, three H-bonds were found; one was formed between the hydroxyl group at C-14 and T797 (distance 1.69 Å), one was formed between the aldehyde group at C-10 and Q111 (distance 1.89 Å), and the other one was formed between the hydroxyl group at C-2′ and Q111 (distance 2.15 Å). In accord with the comparable Na^+,K^+-ATPase inhibitory potency of compounds **18** and **20** (Table 3), similar intermolecular interaction was observed when compound **18** was replaced with compound **20** in the docking simulation though more H-bonds were observed. Six H-bonds were found: three were formed between the hydroxyl group at C-14 and T797/D121 (distances 1.75, 1.88, and 2.13 Å, respectively), one was formed between the aldehyde group at C-10 and Q111 (distance 1.87 Å), and the other two were formed between E116 and the hydroxyl groups at C-2′ and C-3′ (distances 1.87 and 1.93 Å). However, the three H-bonds formed with the hydroxyl group at C-14 of compound **20** were relatively weak in comparison with the strong H-bond (short distance of 1.69 Å) formed with the hydroxyl group at C-14 of compound **18**. To compare relative binding affinities of compounds 2, 18 and 20 in the binding cavity of Na^+,K^+-ATPase, LigScore 1 and 2 were calculated. The results showed that LigScore 1 were 5.22, 5.75 and 6.13 while LigScore 2 were 6.13, 7.38 and 6.61 for compounds **2**, **18** and **20**, respectively. On the basis of the LigScore calculations (average 5.675, 6.515 and 6.370 for **2**, **18** and **20**), the binding affinity of compound **2** was apparently lower than those of compounds **18** or **20**, and compounds **18** and **20** were likely to possess similar binding affinity. The theoretical calculation might partly explain why compound **18** and compound **20** possessed comparable inhibitory potency on Na^+,K^+-ATPase. Taken together, the relatively strong H-bond interaction and high binding affinity in the binding cavity seemed to explain why compounds **18** and **20** possessed higher inhibitory potency on Na^+,K^+-ATPase than compound **2**. Detailed intermolecular H-bond geometries in the docking simulation of compounds **2**, **18**, and **20** were shown in Table S1 (ESI†).

Conclusions

In summary, this paper describes the isolation and structure elucidation of five new cardenolide lactates and one dioxane double linked cardenolide glycoside along with 15 known compounds from the ornamental milkweed *Asclepias curassavica*. The structures and absolute stereochemistry were elucidated by NMR spectroscopic data, and were confirmed by ORD spectral data as well as X-ray crystallographic analysis. Simultaneous isolation of dioxane double linked cardenolide glycosides and cardenolide lactates provided unique chemotaxonomic markers for this genus. The dioxane double linked cardenolide glycosides showed the most potent cytotoxic effect against DU145 cancer cells followed by normal cardenolides and cardenolide lactates, while the C21 steroids were non-cytotoxic. Enzymatic assay established a correlation between the cytotoxic effect and the inhibitory effect on Na^+,K^+-ATPase. Molecular docking analysis revealed strong H-bond interactions in the binding cavity of dioxane double linked cardenolide glycosides.

Experimental section

General

Melting points were measured on an X-5 melting point apparatus without correction. Optical rotations were determined using MeOH solutions on a Jasco P-1020 polarimeter at room temperature. UV spectra were measured with a Jasco V-550 UV/VIS spectrophotometer, while IR spectra were collected from a Jasco FTIR-480 Plus spectrometer. NMR spectra were obtained on a Bruker AV-400 spectrometer. ESIMS and HRESIMS spectra were obtained on a Finnigan LCQ Advantage Max ion trap mass spectrometer and an Agilent 6210 ESI/TOF mass spectrometer, respectively. Silica gel for column chromatography (200–300 mesh) was produced by Qingdao Marine Chemical Industrials, and Sephadex LH-20 was purchased from Pharmacia Biotech (Pharmacia, Kalamazoo, MI, USA). Precoated silica gel GF_{254} plates (Qingdao Marine Chemical Plant, Qingdao, P. R. China) were used for TLC analysis. Preparative HPLC was performed on a Varian Prostar system equipped with a preparative Cosmosil C_{18} column (5 μm, 20 × 250 mm) column.

Plant material

The whole plants of *Asclepias curassavica* were collected in Zhongshan city of Guangdong province, P. R. China in August 2012, and authenticated by Prof. Guang-Xiong Zhou (Jinan University). A specimen (no. 2012081001) was deposited in the Institute of Traditional Chinese Medicine and Natural Products, College of Pharmacy, Jinan University, P. R. China.

Extraction and isolation

The dried and powdered whole plants of *Asclepias curassavica* (20 kg) were extracted with 70% (V/V) ethanol at 90 °C. The solution was concentrated under reduced pressure to afford a crude extract (3 kg), which was subsequently partitioned between EtOAc and H_2O. The EtOAc extract (200 g) was subjected to silica gel column chromatography eluted with gradient mixtures of $CHCl_3$–MeOH (100 : 0→1 : 4) to yield 18 fractions (Fr. 1 to Fr. 18).

Fr. 9 (18 g) was subjected to silica gel column chromatography, eluted with a gradient $CHCl_3$–CH_3OH (from 30 : 1 to 1 : 1) system to give seven subfractions (Fr. 9A to Fr. 9G). Fr. 9E was subjected to preparative HPLC eluted by CH_3CN–H_2O (7 : 3) to afford compounds **1** (34 mg), **2** (18 mg) and **16** (39 mg). Fr. 12 (18 g) was subjected to silica gel column chromatography eluted with gradient mixtures of CH_3Cl–MeOH

(20 : 0→1 : 4) to yield ten subfractions (Fr. 12A to Fr. 12J). Subfraction Fr. 12E (2.8 g) was separated by Sephadex LH-20 and preparative HPLC eluted by CH_3CN–H_2O (70 : 30) to yield compounds **6** (24 mg), **9** (23 mg) and **12**(18 mg). Subfraction Fr. 12H was purified by preparative HPLC eluted by CH_3CN–H_2O (70 : 30) to afford **3** (59 mg) **13** (24 mg) and **15** (23 mg). Subfraction Fr.12G (320 mg) was re-separated by Sephadex LH-20 column (CH_3OH) and preparative HPLC [CH_3CN–H_2O (70 : 30)] to yield compounds **18** (27 mg) and **19** (21 mg). Subfraction Fr.12H was purified by preparative HPLC [CH_3CN–H_2O (70 : 30)] to give **4** (26 mg), **20** (27 mg) and **21** (20 mg). Fr. 15 (36 g) was subjected to ODS column chromatography eluted with gradient mixtures of MeOH–H_2O (1 : 4→4 : 1) to yield 13 subfractions (Fr. 15A to Fr. 15M). Subfraction Fr.15F was subjected to preparative HPLC eluted by CH_3CN–H_2O (70 : 30) to afford compounds **7** (34 mg), **8** (18 mg) and **10** (13 mg). Subfraction Fr.15H was purified by preparative HPLC eluted by CH_3CN–H_2O (70 : 30) to give **5** (21 mg), **11** (24 mg) and **14** (23 mg). Fr. 18 (28 g) was subjected to silica gel column chromatography, eluted with a $CHCl_3$–CH_3OH gradient system (30 : 1–1 : 1) to give 10 fractions (Fr. 15A to Fr. 15J). Subfraction Fr.15E was subjected to preparative HPLC [CH_3CN–H_2O (7 : 3)] to give compound **17** (30 mg).

(3*R*,5*S*,8*R*,9*S*,10*S*,13*R*,14*S*,17*R*,20*Z*,2′*S*)-3-*O*-Urarigenin lactate (1). Colorless crystals from MeOH; $[\alpha]_D^{25}$ −49 (0.1, $CHCl_3$); UV (MeOH) λ_{max} (log ε) 217(4.05) nm; IR (KBr) ν_{max} 3430, 2939, 1733, 1716 cm^{-1}; ^1H and ^{13}C NMR data, see Table 1; HRESIMS *m*/*z* 469.2563 $[M + Na]^+$ (calcd for $C_{26}H_{37}O_6Na$, 469.2561).

(3*R*,5*S*,8*R*,9*S*,10*S*,13*R*,14*S*,17*R*,20*Z*,2′*R*)-3-*O*-Urarigenin lactate (2). Colorless crystals; $[\alpha]_D^{25}$ −67 (0.1, MeOH); UV (MeOH) λ_{max} (log ε) 216 (4.24) nm; IR (KBr) ν_{max} 3412, 2939, 1733, 1717 cm^{-1}; ^1H and ^{13}C NMR data, see Table 1; HRESIMS *m*/*z* 447.2745 $[M + H]^+$ (calcd for $C_{26}H_{38}O_6$, 447.2741).

(3*S*,5*S*,8*R*,9*S*,10*R*,13*R*,14*S*,17*R*,20*Z*,2″*S*)-19-*O*-Coroglaucigenin lactate (3). Colorless crystals; $[\alpha]_D^{25}$ −67 (0.1, MeOH); UV (MeOH) λ_{max} (log ε) 218 (4.16) nm; IR (KBr) ν_{max} 3469, 2930, 1733, 1714 cm^{-1}; ^1H and ^{13}C NMR data, see Table 1; HRESIMS *m*/*z* 463.2677 $[M + Na]^+$ (calcd for $C_{26}H_{39}O_7$, 463.2690).

(3*S*,5*S*,8*R*,9*S*,10*R*,13*R*,14*S*,17*R*,20*Z*,2′*R*,2″*S*)-3,19-*O*-Coroglaucigenin dilactate (4). Colorless powder; $[\alpha]_D^{25}$ −46 (0.1, MeOH); UV (MeOH) λ_{max} (log ε) 218 (4.08) nm; IR (KBr) ν_{max} 3446, 2932, 1733, 1711 cm^{-1}; ^1H and ^{13}C NMR data, see Table 1; HRESIMS *m*/*z* 557.2448 $[M + Na]^+$ (calcd for $C_{29}H_{41}O_9Na$, 534.2451).

(3*R*,5*S*,8*R*,9*S*,10*R*,13*R*,14*S*,17*R*,20*Z*,2″*R*)-19-*O*-Frugoside lactate (5). Colorless powder; $[\alpha]_D^{25}$ −54 (0.1, MeOH); UV (MeOH) λ_{max} (log ε) 217 (4.17); IR (KBr) ν_{max} 3446, 2934, 1733 cm^{-1}; ^1H and ^{13}C NMR data, see Table 1; HRESIMS *m*/*z* 608.2531 $[M + H]^+$ (calcd for $C_{32}H_{48}O_{11}$).

(2*R*,3*R*,5*S*,8*R*,9*S*,10*R*,13*R*,14*S*,17*R*,20*Z*,1′*S*,2′*S*,3′*S*,5′*R*)-19β-Oxhydrylcalotropin (17). Colorless crystals from MeOH solution; $[\alpha]_D^{25}$ −49 (0.1, MeOH); UV (MeOH) λ_{max} (log ε) 205(2.59) nm; IR (KBr) ν_{max} 3420, 1725 cm^{-1}; ^1H and ^{13}C NMR data, see Table 1; HRESIMS *m*/*z* 521.2581 $[M + H]^+$ (calcd for $C_{28}H_{40}O_9$, 521.2589).

The hydrolysis of compounds 4 and 5

Compounds **4** (3.012 mg) and **5** (3.734 mg) were submitted to hydrolysis by adding to a solution of NaOH in MeOH (0.5 N, 4 mL). The mixture was stirred for 10 hours at room temperature (no **4** or **5** was detected by TLC analysis). After the reaction, the mixture was acidified with dilute HCl (4%) to pH 5–6 and saturated with NaCl, followed by extraction with $CHCl_3$. Then the aqueous layer was concentrated *in vacuo* and the residue was dissolved in 0.5 mL water. The optical rotation of an aliquot of the aqueous solution (200 μL) containing the lactic acid (c = 0.195 for **4** and 0.111 for **5**) was determined using a Jasco P-1020 spectrometer (l = 0.1 dm).

X-ray analysis

X-ray diffraction data were collected on an Agilent Gemini S ultra spharrie CCD diffractometer using graphite monochromated radiation (λ = 1.54178 Å) under room temperature. The crystal structures were elucidated by direct methods using SHELXS-97 and refined by full-matrix least-squares method on F^2 using SHELXS-97. In the structure refinement, non-hydrogen atoms were refined anisotropically. Hydrogen atoms bonded to carbons were placed at their geometrically ideal positions. Hydrogen atoms bonded to oxygen were located by employing the difference Fourier method and were included in the calculation of structure factors with isotropic temperature factors.

(3*R*,5*S*,8*R*,9*S*,10*S*,13*R*,14*S*,17*R*,20*Z*,2′*S*)-3-*O*-Urarigenin lactate (1). Colorless columnar crystals from MeOH, $C_{26}H_{38}O_6$, orthorhombic, $P2_12_12_1$, a = 11.4718(5), b = 12.9514(5), c = 15.8446(8) Å, β = 90.0, V = 2354.13(18) $Å^3$, Z = 4, d_x = 1.260 Mg m^{-3}, μ(CuKα) = 0.711 mm^{-1}, F(000) = 968. 3588 unique reflections were collected to θ_{max} = 62.76°, in which 3276 reflections were observed [$F^2 > 4\sigma(F^2)$]. The final R = 0.0353, Rw = 0.0873, S = 1.062 and CCDC 1014923.

(3*R*,5*S*,8*R*,9*S*,10*S*,13*R*,14*S*,17*R*,20*Z*,2′*R*)-3-*O*-Urarigenin lactate (2). Colorless columnar from MeOH, $C_{26}H_{38}O_6$, orthorhombic, $P2_12_12_1$, a = 10.4301(3), b = 11.8072(3), c = 18.7440(5) Å, β = 90.0, V = 2308.33(11) $Å^3$, Z = 4, d_x = 1.325 Mg m^{-3}, μ(CuKα) = 0.755 mm^{-1}, F(000) = 996. 3400 unique reflections were collected to θ_{max} = 62.74°, in which 3514 reflections were observed [$F^2 > 4\sigma(F^2)$]. The final R = 0.0315, Rw = 0.0810, S = 1.065 and CCDC 1014924.

(3*S*,5*S*,8*R*,9*S*,10*R*,13*R*,14*S*,17*R*,20*Z*,2″*S*)-19-*O*-Coroglaucigenin lactate (3). Colorless columnar from MeOH, $C_{26}H_{38}O_7$, monoclinic, $P2_1$, a = 6.3498(3), b = 19.5019(8), c = 9.5651(5) Å, β = 102.297(4), V = 1157.30(9) $Å^3$, Z = 2, d_x = 1.327 Mg m^{-3}, μ(CuKα) = 0.776 mm^{-1}, F(000) = 500. 2600 unique reflections were collected to θ_{max} = 62.66°, in which 2721 reflections were observed [$F^2 > 4\sigma(F^2)$]. The final R = 0.0310, Rw = 0.0783, S = 1.057 and CCDC 1014925.

(2*R*,3*R*,5*S*,8*R*,9*S*,10*R*,13*R*,14*S*,17*R*,20*Z*,1′*S*,2′*S*,3′*S*,5′*R*)-19β-Hydroxycalotropin (17). Colorless crystals from MeOH, $C_{28}H_{40}O_9{\cdot}4H_2O$, monoclinic, $P2_1$, a = 8.9982(4), b = 12.3600(7), c = 13.3864(8) Å, β = 98.572(5), V = 1472.17(14) $Å^3$, Z = 2, d_x = 1.319 Mg m^{-3}, μ(CuKα) = 0.882 mm^{-1}, F(000) = 624. 3354

unique reflections were collected to θ_{max} = 62.65°, in which 2798 reflections were observed [$F^2 > 4\sigma(F^2)$]. The final R = 0.0459, wR_2 = 0.1181, S = 1.107 and CCDC 1014926.

Cytotoxicity assay

The MTT assay was done as described previously[30] with taxol served as the positive control. Briefly, the prostate cancer cells were plated into 96-well plates at a density of 3×10^3 cells per well for androgen independent cells DU145. Cells were maintained in RPMI-1640 medium supplemented with 10% fetal bovine serum (Gibco, Rockville, MD, USA), 100 units mL^{-1} penicillin and streptomycin at 37 °C in a 5% CO_2 humidified atmosphere. Following incubation for 48 h, 20 μL of the MTT solution [5 mg mL^{-1} in phosphate buffered saline (PBS)] was added to each well, and the cells were further incubated for 4 h. Then the medium was removed and replaced by 150 μL of DMSO in each well to dissolve the formazan crystals. The relative cell viability was determined by measuring the optical densities at 570 nm on microplate reader (SPECTRAmax 250, Molecular Devices, Minnesota, USA), and was expressed as a percentage relative to the control. The experiments were performed three times, each in triplicate.

Na^+,K^+-ATPase inhibition assay

Na^+,K^+-ATPase from pig kidney microsomal membranes was prepared by treatment with SDS and purified by differential centrifugation.[31] The specific activity of the enzyme preparation was approximately 30 μmol ATP hydrolysed per mg protein per min at 37 °C.[31,32] The Na^+,K^+-ATPase inhibitory activities of **2**, **3**, **8**, **10**, and **18–21** were determined essentially as previously reported.[26] In brief, Na^+,K^+-ATPase is incubated at 37 °C for 2 hours in the presence of 3 mM $MgCl_2$, 3 mM Na-phosphate and 40 mM Tris (pH 7.0) with increasing concentrations of inhibitor. The Na^+,K^+-ATPase activity is subsequently determined by 40-fold dilution into a standard assay medium containing 130 mM NaCl, 20 mM KCl, 4 mM $MgCl_2$ and 3 mM ATP (in triplicate). For each inhibitor concentration the inactivation was determined in two or three independent experiments and the error bars in Fig. S46† indicate the standard deviation. Data in Fig. 46S† are given as percent of the Na^+,K^+-ATPase activity in the absence of inhibitor (see legend to Fig. S46† for details).

The inhibitors were solubilised in DMSO as concentrated solutions, typically as 10 mM solutions. The dilution into the Na^+,K^+-ATPase incubation medium was at least 40-fold, giving a maximal DMSO concentration of 2.5% in the incubation medium. Control experiments showed that incubation for 2 hours at 37 °C as above with 2.5% DMSO (absence of inhibitor) led to less than 10% inhibition of Na^+,K^+-ATPase activity.

Molecular modeling and docking

The crystal structure of pig kidney Na^+,K^+-ATPase-ouabain complex with Mg^{2+} (PDB code 4HYT) were downloaded from Protein Data Bank.[29] Ouabain in this complex structure was removed first, and the modified Na^+,K^+-ATPase after hydrogen saturation was applied with CHARMm force field[33] using the Discover Studio 2.1 package (http://accelrys.com/products/discovery-studio/). The 2D structures of steroid-like compounds used in this study were constructed by using the ChemDraw program, and their corresponding 3D structures were converted by the Chem3D program (http://www.cambridgesoft.com/). The binding site for the steroid-like compounds in the Na^+,K^+-ATPase subunit was defined as ouabain binding site among the extracellular loops linking transmembrane segments in the ouabain-Na^+,K^+-ATPase complex structure. In the docking simulation of compounds, the ligand-binding domain was defined as the region of the sphere with a 12.5 Å radius from the center of the binding pocket. The LibDock methodology effectively executed the docking of combinatorial libraries of compounds in a high-throughput manner while keeping the protein structure fixed. In all complex structures generated by LibDock module, the binding orientation and conformation of compounds with the similar ouabain binding mode were selected. The energy of the ligand and residues in the binding site of the selected docking complex structures were further energy-minimized by smart minimize algorithm with CHARMm force field in the Discover Studio 2.1 package.[34] The distances of intermolecular hydrogen bonds (from proton to acceptor) were set as less than 2.5 Å. The binding affinities of compound **2**, **18** and **20** in the binding pocket of Na^+,K^+-ATPase were scored by LigScore 1 and LigScore 2.[35]

Acknowledgements

This work was supported by the 111 Project (no. B13038) from the Ministry of Education of P. R. China.

Notes and references

1 L. Yatime, M. Laursen, J. P. Morth, M. Esmann, P. Nissen and N. U. Fedosova, *J. Struct. Biol.*, 2011, **174**, 296.
2 R. A. Newman, P. Yang, A. D. Pawlus and K. I. Block, *Mol. Interv.*, 2008, **8**, 36.
3 S. B. Malcolm, *Chemoecology*, 1990, **1**, 12.
4 S. M. Kupchan, J. P. Knox, J. E. Kelsey and J. A. Saenzrenauld, *Science*, 1964, **146**, 1685.
5 F. Abe, Y. Mori and T. Yamauchi, *Chem. Pharm. Bull.*, 1991, **39**, 2709.
6 M. C. Roy, F. R. Chang, H. S. Huang, M. Y. N. Chiang and Y. C. Wu, *J. Nat. Prod.*, 2005, **68**, 1494.
7 J. Z. Li, C. Qing, C. X. Chen, X. J. Hao and H. Y. Liu, *Med. Chem. Lett.*, 2009, **19**, 1956.
8 H. T. A. Cheung and C. J. Nelson, *J. Chem. Soc., Perkin Trans. 1*, 1989, 1563.
9 Y. L. Liu and P. M. Loshkarev, *Meditsinskaya Promyshlennost SSSR*, 1963, **17**, 18.
10 F. Kiuchi, Y. Fukao, T. Maruyama, T. Obata, M. Tanaka, T. Sasaki, M. Mikage, M. E. Haque and Y. Tsuda, *Chem. Pharm. Bull.*, 1998, **46**, 528.

11 T. Reichstein, A. M. Kuritzkes, Ch. Tamm and H. Jaeger, *Helv. Chim. Acta*, 1963, **46**, 8.
12 D. H. G. Crout, R. F. Curtis, C. H. Hassall and T. L. Jones, *Tetrahedron Lett.*, 1963, 63.
13 R. M. Padua, A. B. Oliveira, J. D. S. Filho, G. J. Vieira, J. A. Takahashi and F. C. Braga, *J. Brazil. Chem. Soc.*, 2005, **16**, 614.
14 X. Y. Li, H. X. Sun, Y. P. Ye, F. Y. Chen, J. Tu and Y. J. Pan, *Chem. Biodiversity*, 2005, **2**, 1701.
15 J. Z. Li, H. Y. Liu, Y. J. Lin;, X. J. Hao, W. Ni and Ch. X. Chen, *Steroids*, 2008, **73**, 594.
16 H. T. A. Cheung, C. J. Nelson and T. R. Watson, *J. Chem. Sci.*, 1988, **7**, 1851.
17 J. Z. Li, C. Qing, C. X. Chen, X. J. Hao and H. Y. Liu, *Bioorg. Med. Chem. Lett.*, 2009, **19**, 1956.
18 H. T. A. Cheung and T. R. Watson, *J. Chem. Soc.*, 1980, 2162.
19 H. T. A. Cheung, F. C. K. Chiu, T. R. Watson and R. J. Wells, *J. Chem. Soc., Perkin Trans.*, 1983, 2827.
20 S. D. Jolad, R. B. Bates, J. R. Cole, J. J. Hoffmann, T. J. Siahaan and B. N. Timmermann, *Phytochemistry*, 1986, **25**, 2581.
21 K. Koike, C. Bevelle, S. K. Talapatra, G. A. Cordell and N. R. Farnsworth, *Chem. Pharm. Bull.*, 1980, **28**, 401.
22 B. C. Chao and J. L. Xu, *Food Fermentation Ind.*, 1993, **3**, 56.
23 I. M. Mujtaba, E. A. Edreder and M. Emtir, *Appl. Energy*, 2012, **89**, 74.
24 G. A. Fleming, K. T. Murray, C. Yu, J. G. Byrne, J. P. Greelish, M. R. Petracek, S. J. Hoff, S. K. Ball, N. J. Brown and M. Pretorius, *J. Am. Heart Assoc.*, 2008, **118**, 1619.
25 A. A. Agrawal, G. Petschenka, R. A. Bingham, M. G. Weber and S. Rasmann, *New Phytol.*, 2012, **194**, 28.
26 D. A. Middleton, S. Rankin, M. Esmann and A. Watts, *Proc. Natl. Acad. Sci. U. S. A.*, 2000, **97**, 13602.
27 H. Ogawa, T. Shinoda, F. Cornelius and C. Toyoshima, *Proc. Natl. Acad. Sci. U. S. A.*, 2009, **106**, 13742.
28 F. Cornelius, R. Kanai and C. Toyoshima, *J. Biol. Chem.*, 2013, **288**, 6602.
29 M. Laursen, L. Yatime, P. Nissen and N. U. Fedosova, *Proc. Natl. Acad. Sci. U. S. A.*, 2013, **110**, 10958.
30 T. Mosmann, *J. Immunol. Methods*, 1983, **65**, 55.
31 I. Klodos, M. Esmann and R. L. Post, *Kidney Int.*, 2002, **62**, 2097.
32 M. Esmann, *Methods Enzymol.*, 1988, **156**, 105.
33 B. R. Brooks, R. E. Bruccoleri, B. D. Olafson, D. J. States, S. Swaminathan and M. Karplus, *J. Comput. Chem.*, 1983, **4**, 187.
34 S. L. Dixon and K. M. Merz Jr., *J. Med. Chem.*, 2001, **44**, 3795.
35 S. L. Mayo, B. D. Olafson and W. A. Goddard, *J. Phys. Chem.*, 1990, **94**, 8897–8909.